BOREAL ENVIRONMENT RESEARCH 21: 319–331
ISSN 1239-6095 (print) ISSN 1797-2469 (online)

Helsinki 23 May 2016

On the mode-segregated aerosol particle number concentration load: contributions of primary and secondary particles in Hyytiälä and Nanjing

Markku Kulmala[1], Krista Luoma[1], Aki Virkkula[2,3,4], Tuukka Petäjä[1,2], Pauli Paasonen[1], Veli-Matti Kerminen[1], Wei Nie[1,2,4], Ximeng Qi[2,4], Yicheng Shen[2,4], Xuguang Chi[2,4] and Aijun Ding[2,4]

[1)] *Department of Physics, P.O. Box 64, FI-00014 University of Helsinki, Finland*
[2)] *Finnish Meteorological Institute, Research and Development, FI-00101 Helsinki, Finland*
[3)] *Joint International Research Laboratory of Atmospheric and Earth System Sciences & School of Atmospheric Sciences, Nanjing University, 210023 Nanjing, China*
[4)] *Institute for Climate and Global Change Research & School of Atmospheric Sciences, Nanjing University, 210023 Nanjing, China*

Received 26 Jan. 2016, final version received 18 Mar. 2016, accepted 18 Mar. 2016

Kulmala M., Luoma K., Virkkula A., Petäjä T., Paasonen P., Kerminen V.-M., Nie W., Qi X., Shen Y., Chi X. & Ding A. 2016: On the mode-segregated aerosol particle number concentration load: contributions of primary and secondary particles in Hyytiälä and Nanjing. *Boreal Env. Res.* 21: 319–331.

Aerosol particle concentrations in the atmosphere are governed by their sources and sinks. Sources include directly-emitted (primary) and secondary aerosol particles formed from gas-phase precursor compounds. The relative importance of primary and secondary aerosol particles varies regionally and with time. In this work, we investigated primary and secondary contributions to mode-segregated particle number concentrations by using black carbon as a tracer for the primary aerosol number concentration. We studied separately nucleation, Aitken and accumulation mode concentrations at a rural boreal forest site (Hyytiälä, Finland) and in a rather polluted megacity environment (Nanjing, China) using observational data from 2011 to 2014. In both places and in all the modes, the majority of particles were estimated to be of secondary origin. Even in Nanjing, only about half of the accumulation mode particles were estimated to be of primary origin. Secondary particles dominated particularly in the nucleation and Aitken modes.

Introduction

Primary particle emissions (Paasonen *et al*. 2016) and new particle formation (NPF) (Kulmala *et al*. 2004, Kulmala and Kerminen 2008) together with wet and dry removal processes and coagulation scavenging (Farmer *et al*. 2013, Schutgens and Stier 2014, Tsigaridis *et al*. 2014) determine the atmospheric aerosol particle number load. In a modeling framework, the differentiation of sources is straightforward and the relative contributions of primary and secondary sources can be estimated based on emission inventories and modeled meteorology and chemical transformation (e.g. Fontoukis *et al*. 2012, Posner and Pandis 2015). Global model studies suggest that atmospheric NPF is the dominant source of the particle number load (Yu *et al*. 2010, Makkonen *et al*.

Editor in charge of this article: Hannele Korhonen

2012), and an important source of cloud condensation nuclei (e.g. Merikanto *et al*. 2009, Kerminen *et al*. 2012), in the global troposphere. In continental boundary layers, the relative contributions of primary and secondary particle sources appear to be quite variable, and rather uncertain due to several assumptions inherent to current modeling frameworks (Spracklen *et al*. 2010, Reddington *et al*. 2011, Posner and Pandis 2015).

Observational studies of primary and secondary aerosol particle sources are still rather limited, especially in terms of their spatial and temporal extend (e.g. Brines *et al*. 2015). Experimental methods for the source apportionment typically assume that primary and secondary aerosols can be separated based on their chemical signatures (e.g. Docherty *et al*. 2008, Jimenez *et al*. 2009, Yatavelli *et al*. 2015). Rodríguez and Cuevas (2007) presented a methodology, in which the concentration of primary traffic-related aerosol particles, N_1, is estimated from measured black (BC) carbon concentrations, [BC], using the relation

$$N_1 = S_1 \times [\mathrm{BC}], \quad (1)$$

where S_1 is the semi-empirical scaling factor derived from concurrent observations of the total aerosol number concentration and BC concentration. Since the total particle number concentration (N) is the sum of primary (N_1) and secondary (N_2) particles, the number concentration of secondary particles is obtained from the residual:

$$N_2 = N - N_1. \quad (2)$$

The limitations of this method have been discussed in detail by Rodríguez and Cuevas (2007) and Reche *et al*. (2011), and will be returned to when comparing our results with other studies employing the same approach.

The aim of this study was to explore the relative contributions of primary and secondary sources to the total and mode-segregated particle number concentrations in two distinctively different environments. For this purpose, we utilized Eqs. 1 and 2 not only to the total particle number concentration, as done in previous investigations, but also to different particle size ranges or modes. The work relied on observations made in Hyytiälä (Finland) and Nanjing (China). Based on previous research (e.g. Kulmala *et al*. 2013, Ding *et al*. 2013a), Hyytiälä represents an environment where biogenic secondary aerosol particles dominate total particle number concentrations, whereas Nanjing is presumably a location where anthropogenic particle sources are more pronounced.

Material and methods

We performed BC and aerosol number size distribution measurements at the Station for Measuring Ecosystem–Atmosphere Relations (SMEAR II; *see* Hari and Kulmala 2005) station in Hyytiälä, Finland, and at the Station for Observing Regional Processes of the Earth System (SORPES, Ding *et al*. 2013a) in Nanjing, China. The observation periods used in the analysis conducted here were 1 Jan. 2011–22 Oct. 2014 for SMEAR II (76 628 data points representing 10-min averages) and 28 Apr. 2013–6 Aug 2014 for SORPES (24 418 data points).

Observation sites

The SMEAR II station is located in Hyytiälä (61°51´N, 24°17´E, 181 m a.s.l.), southern Finland, in the middle of a boreal forest, surrounded by a fairly homogeneous Scots pine (*Pinus sylvestris*) population. Areas to the north and northeast are comprised of small lakes and wetlands. The station was opened in 1995 and has been providing research facilities to many researchers ever since. Hyytiälä has a comprehensive measurement set-up for the observations of the ecosystem–atmosphere interactions. It is located about 60 km NE from the third largest city in Finland, Tampere. Most pollution transported to the measurement site originate either from the Tampere area or from the saw mill located in Korkeakoski, about 10 km SE from SMEAR II. Detailed information on the SMEAR II station can be found in Hari and Kulmala (2005).

In Nanjing, China, the measurements were conducted at the SORPES station (118°57´E, 32°07´N, 40 m above mean sea level) in the Xianlin campus of the Nanjing University. The site is a suburban background station, with a little

influence from local emissions yet in the middle of heavy regional pollution (Ding *et al*. 2013a, 2013b, Herrmann *et al*. 2014, Xie *et al*. 2015).

Instrumentation

Aerosol number size distributions were measured with a Differential Mobility Particle Sizer (DMPS) in both Hyytiälä and Nanjing. The time resolution of the instrument was 10 min. More detailed descriptions of the aerosol instrumentation used at the SMEAR II and SORPES stations can be found in Aalto *et al*. (2001) and Qi *et al*. (2015), respectively. The measured particle number size distributions were divided into three modes according to the particle size: the nucleation mode (particle diameter in the range 3–25 nm), Aitken mode (25–100 nm) and accumulation mode (100–1000 nm).

At the SMEAR II station, BC concentrations were measured with a Magee Scientific 7-wavelength aethalometer (AE-31) and with a Multiangle Absorption Photometer (MAAP) at a 5 min averaging time. At the SORPES station, BC concentrations were measured with a 7-wavelength aethalometer (AE-31) (Virkkula *et al*. 2015). At SMEAR II the sample air to the optical instruments was taken through a common PM_{10} inlet. At SORPES there were two separate inlets: the nephelometer had a PM_{10} inlet and aethalometer had a $PM_{2.5}$ inlet.

In order to process aethalometer data, also scattering coefficient (σ_{sp}) measurements are needed. At SMEAR II, σ_{sp} was measured with a TSI model 3565 nephelometer at the wavelengths λ = 450, 550, and 700 nm (Virkkula *et al*. 2011), and at SORPES it was measured with an Ecotech Aurora 3000 nephelometer at λ = 450, 525 and 635 nm (Virkkula *et al*. 2015). The data were corrected for truncation according to Anderson and Ogren (1998) and Müller *et al*. (2011a), and then interpolated and extrapolated to the aethalometer wavelengths. In addition to deriving scattering-corrected BC concentrations, σ_{sp} was used to calculate the single-scattering albedo $\omega_0 = \sigma_{sp}/(\sigma_{sp} + \sigma_{ap})$, where σ_{sp} is the absorption coefficient.

In this study, only the data which were collected when the relative humidity (RH) of the sample air was < 50% were used. At higher RH values particles grow notably in size and affect all optical measurements. The World Meteorological Organization Global Atmosphere Watch (WMO/GAW) recommends for aerosol monitoring stations to keep RH of the sample air at 45% ± 5% (WMO 2003).

Data processing of the BC measurements

The aethalometer reports BC mass concentrations calculated from the rate of change of light attenuation, but it is well known that its signal is also affected by scattering aerosol and that the relationship varies with the loading of the filter. Various methods for correcting for these have been developed (e.g. Weingartner *et al*. 2003, Arnott *et al*. 2005, Virkkula *et al*. 2007, Collaud Coen *et al*. 2010). Of these methods, the ones of Arnott *et al*. (2005) and Collaud Coen *et al*. (2010) take the scattering coefficients explicitly into account. Therefore, we used those two algorithms to calculate σ_{ap} at the aethalometer wavelengths. In those algorithms, the multiple scattering correction factor was set to equal 4.12 for the Arnott *et al*. (2005) version, and to equal 4.26 for the Collaud Coen *et al*. (2010) version, as obtained for the Cabauw data by Collaud Coen *et al*. (2010).

We calculated the corrected BC concentrations from [BC] = σ_{ap}/MAC, where MAC is the mass absorption coefficient. The firmware of the MAAP uses the value of MAC = 6.6 m^2 g^{-1}. It measures σ_{ap} at λ = 637 nm (Müller *et al*. 2011b), so to keep the results of the two methods as comparable as possible, we used the aethalometer data at λ = 660 nm here. We assumed that MAC depends inversely on wavelength, so we used the value of MAC (λ = 660 nm) = 6.4 m^2 g^{-1} for converting σ_{ap} to the BC concentrations.

Results and discussion

General results and comparison to earlier studies

While particle number and BC concentrations

during the measurement periods considered here varied considerably at both sites, the typical concentration levels were clearly higher at SORPES than at SMEAR II (Table 1), as expected due to the overall environmental differences between these sites. The median concentrations differed by about an order of magnitude for the accumulation, Aitken and total particle number concentration, and by almost a factor of 20 for the BC concentration.

When looking at the whole measurement data set, the accumulation mode particle number concentration correlated strongly or moderately with the BC concentration at the two sites (Table 2), whereas the Aitken and nucleation mode particle number concentration had weak or no correlation with [BC]. The weak negative correlation between [BC] and nucleation mode particle number concentrations at SMEAR II can be explained by the fact that atmospheric NPF responsible for most of the nucleation mode particles at this site tends to be associated with clean air masses, with only a marginal contribution from anthropogenic BC sources (e.g. Kulmala *et al*. 2007, Virkkula *et al*. 2011). Because of this negative correlation and of the fact that a very small fraction of the BC particles is in the nucleation mode size range, the division of nucleation mode particles into primary or secondary with the applied method is unreliable.

In the previous studies using Eqs. 1 and 2 to differentiate between primary and secondary particle sources, roughly 1% of the data points in the *N vs*. [BC] scatter plot were located below the line $S_1 \times$ [BC] (e.g. Rodríguez and Cuevas 2007). Because of the ambiguities in determining the value of S_1 that would best scale the primary particle number concentration to the BC concentration, we tested three different constrains to this quantity, namely that 0.2%, 1% or 5% of the data points need to be located below the line $S_1 \times$ [BC] (Fig. 1). We determined S_1 not only for the total particle number concentration, as was done in previous studies, but also for each particle mode separately (Figs. 2 and 3; also the seasonal variation can be seen in those figures).

When using all the data from the two stations, the obtained values of S_1 were greater for SORPES, especially for the accumulation mode, as well as for the total particle number concentration (Table 3). Earlier studies using the same approach for the total particle number concentration have reported values of S_1 ranging between about 3×10^6 and 10×10^6 particles ng(BC)$^{-1}$ (Rodríguez and Cuevas 2007, Fernandez-Camacho *et al*. 2010, Gonzáles *et al*. 2011, Reche *et al*. 2011, Gonzáles and Rodríguez 2013). The reason for the consistently greater values of S_1 in those earlier studies than in our study is unclear, but could be related to the fact that those sites are typically closer to fresh traffic emissions than either SMEAR II or SORPES. Particle growth by coagulation processes during the atmospheric transport from the urban source areas affected by fresh vehicle exhaust emissions to the urban

Table 1. Median and 25th and 75th percentiles of mode-segregated particle number concentrations (cm^{-3}) and black carbon (BC) concentrations (μg m^{-3}) for the periods from 1 Jan. 2011–22 Oct. 2014 in Hyytiälä and 28 Apr. 2013–6 Aug. 2014 in Nanjing.

	25th	Median	75th
SMEAR II			
Nucleation mode	75.1	182	460
Aitken mode	387	703	1230
Accumulation mode	167	330	617
Total concentration	910	1530	2380
BC	0.068	0.135	0.248
SORPES			
Nucleation mode	1000	1700	2870
Aitken mode	4160	6220	9050
Accumulation mode	3390	4980	6960
Total concentration	10200	14200	18900
BC	1.34	2.23	4.02

Table 2. Correlation coefficients (r) for correlations between the BC concentration and particle number concentrations in different modes; in all cases $p < 0.001$.

	Nucleation mode	Aitken mode	Accumulation mode	Total number concentration
SMEAR II	–0.24 (n = 74750)	0.08 (n = 74741)	0.62 (n = 74470)	0.10 (n = 74855)
SORPES	–0.02 (n = 25950)	0.35 (n = 25950)	0.87 (n = 25950)	0.48 (n = 25905)

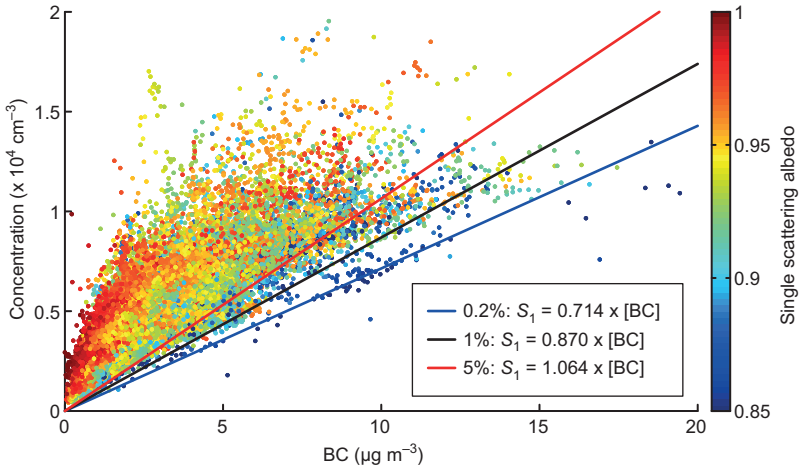

Fig. 1. Accumulation mode number concentration at the SORPES station as a function of BC concentrations illustrates the way, how the value of S_1 is determined. In the constrained fittings, 0.2%, 1% or 5% of the data points are located below the lines determining the values of S_1.

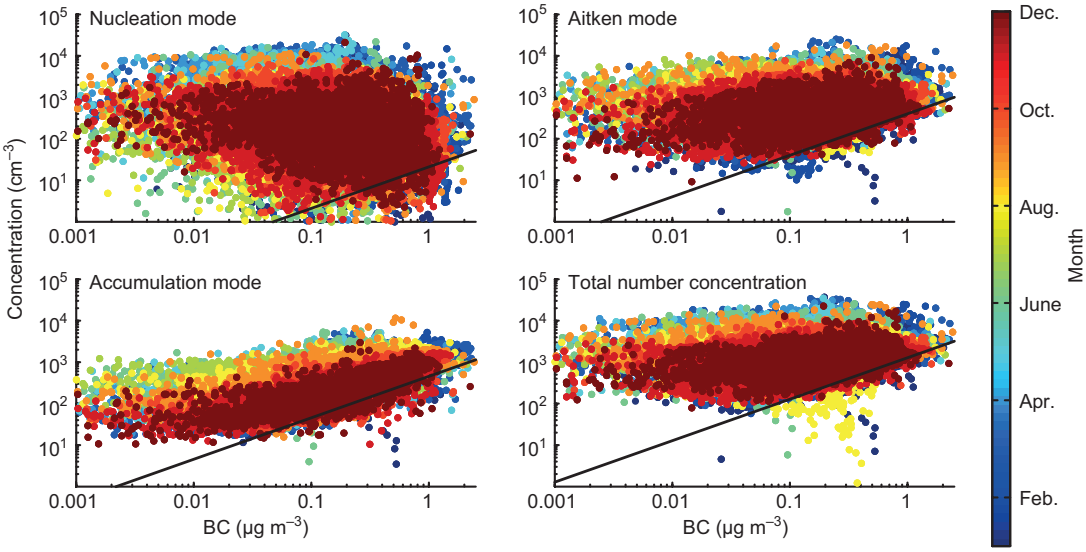

Fig. 2. Particle number concentration as a function of black carbon concentration in the nucleation mode, Aitken mode, accumulation mode and total concentration at the SMEAR II station in Hyytiälä. The lines represent those fittings for S_1 in which 1% of the data points are located below the line.

Table 3. Values of S_1 (10^6 particles ng(BC)$^{-1}$) for different particle modes and total particle number concentrations at SMEAR II and SORPES by assuming that 0.2%, 1% or 5% of the data points in the particle number concentration *vs.* [BC] are below the line $S_1 \times$ [BC].

	Nucleation mode	Aitken mode	Accumulation mode	Total number concentration
SMEAR II				
0.2%	0.007	0.257	0.241	0.638
1%	0.021	0.401	0.457	1.28
5%	0.071	0.768	0.769	2.02
SORPES				
0.2%	0.014	0.327	0.714	1.30
1%	0.037	0.473	0.870	1.67
5%	0.116	0.760	1.06	2.20

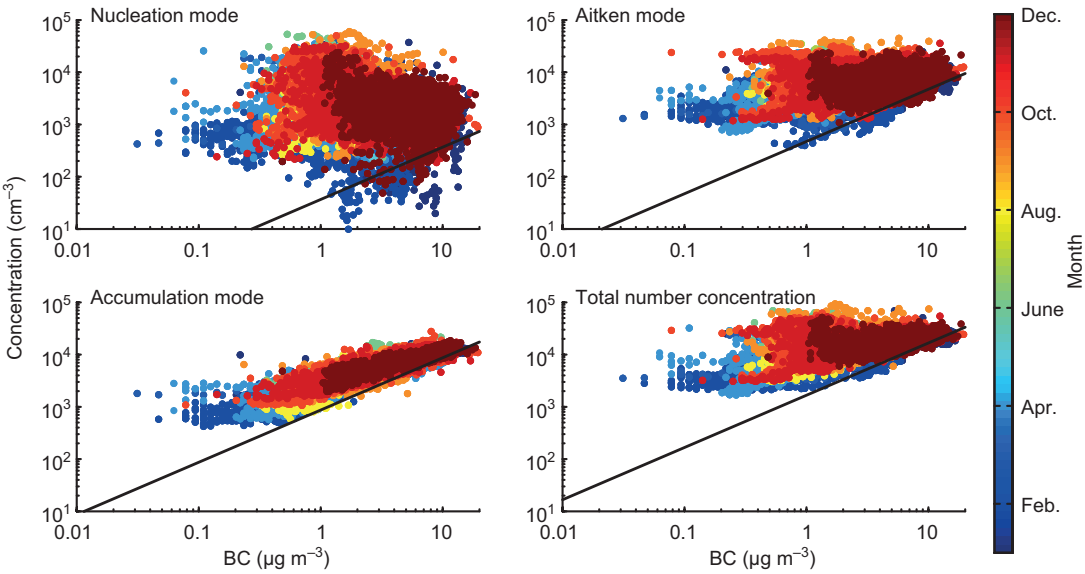

Fig. 3. Particle number concentration as a function of black carbon concentration in the nucleation mode, Aitken mode, accumulation mode and total concentration at the SORPES station in Nanjing.

background (e.g. Nanjing) or rural areas (e.g. Hyytiälä) probably contributed to the decreased value of S_1 observed in this study. The size of the BC cores from fresh traffic emissions is usually rather small compared with that from many other primary particle sources, or in primary particle populations undergone atmospheric aging through coagulation of BC-containing particles (*see* Bond *et al*. 2003 and references therein). A small size of the BC core in primary particles tends to increase the value of S_1. In the next section, we discuss the sensitivity of our results to the assumptions made in treating BC in more detail.

The estimated fraction of primary particles in the Aitken and accumulation modes, as well as in the total particle population, varied by a factor of 2–3 depending on the constraint chosen to determine S_1 (Table 4). In spite of this uncertainty, secondary sources seem to dominate the particle budget at both sites. At the boreal forest site (SMEAR II), primary particles very likely accounted for less than 20% of the total particle population, with a slightly greater share of accumulation mode particles and clearly smaller share of both Aitken and nucleation mode particles. The estimated contribution of primary particles was greater at the polluted urban background site

Table 4. Estimated fraction of primary particles in different modes and total particle population obtained using the values of S_1 given in Table 3. The values obtained for the nucleation mode are very rough estimates (*see* the main text), so these values are given in parentheses.

	Nucleation mode	Aitken mode	Accumulation mode	Total number concentration
SMEAR II				
0.2%	(0.003)	0.05	0.11	0.07
1%	(0.01)	0.08	0.20	0.13
5%	(0.03)	0.16	0.34	0.21
SORPES				
0.2%	(0.02)	0.14	0.41	0.26
1%	(0.04)	0.20	0.50	0.33
5%	(0.12)	0.32	0.60	0.43

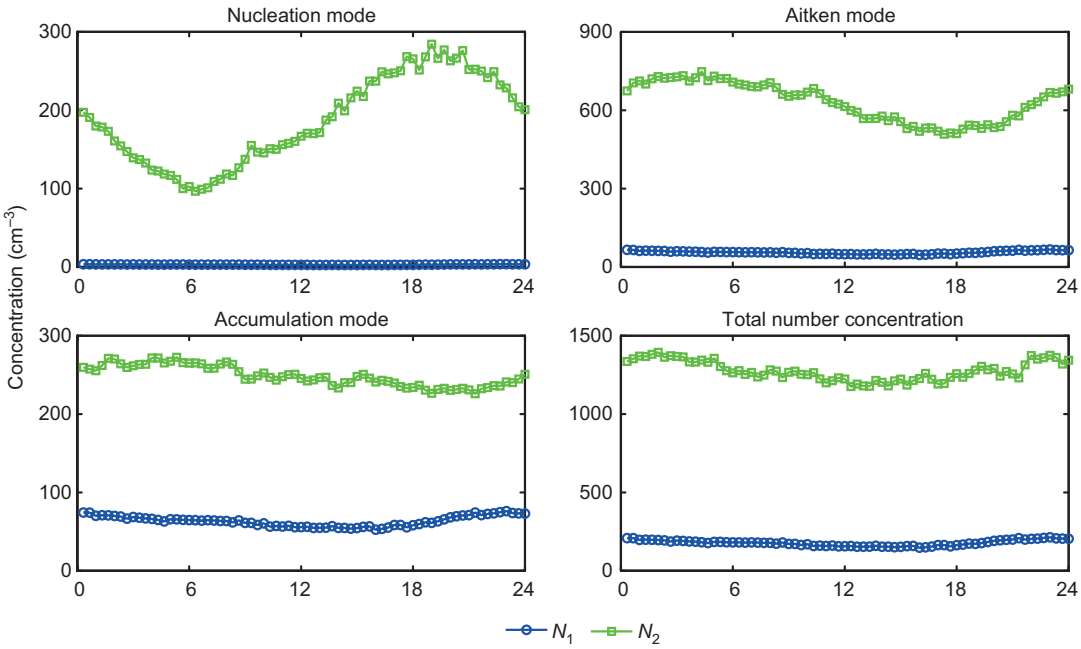

Fig. 4. Diurnal cycles of the primary and secondary source contributions based on hourly median concentrations for the total, nucleation, Aitken and accumulation mode particle number concentration at the SMEAR II station. The division between primary and secondary particles is based on the values of S_1 that assume 1% of the data points to be located between the line determined by $S_1 \times$ [BC].

(SORPES), as one would expect, yet even there the contribution of secondary sourced very likely exceeded 50% for all the particle modes.

It should be noted that the used method erroneously classifies a large fraction of such primary particles that contain little or no BC as secondary particles. Particles belonging to this category include, for example, sea salt and dust particles. These two particle types may account for a notable fraction of the particle mass concentration at both SMEAR II and SORPES, but their contributions to the particle number budgets are expected to be minor. Even some combustion sources produce relatively large primary particles having a very small fraction of BC (e.g. Kleeman *et al*. 1999). Although we could not estimate the contribution of such sources in our data sets, it is very unlikely that such sources would change our main conclusion, i.e. that secondary sources clearly dominate the particle number budget at both sites.

As discussed by Rodríguez and Cuevas (2007), particles formed rapidly during the dilution of a vehicle exhaust into the ambient air make a special case in the methodology applied here. These particles belong mostly to the nucleation mode, partly to the Aitken mode, and contain no BC. Current emission inventories typically consider these particles as primary particles, whereas with Eqs. 1 and 2 they are mainly determined as secondary. As a result, one should be very careful in interpreting the share of primary and secondary nucleation mode particles based on the results given in Table 4.

Finally, we investigated the diurnal behavior of primary and secondary particle concentrations at SMEAR II and SORPES (Figs. 4 and 5). The overall result is that the secondary contribution is greater than the primary one during all times of the day and for all particle size ranges. Only during morning and afternoon rush hours at SORPES, the primary accumulation mode particle number concentration approached the corresponding secondary particle number concentrations.

Sensitivity to the properties of BC

Assuming that the lowest edge of the N_1 *vs*. [BC]

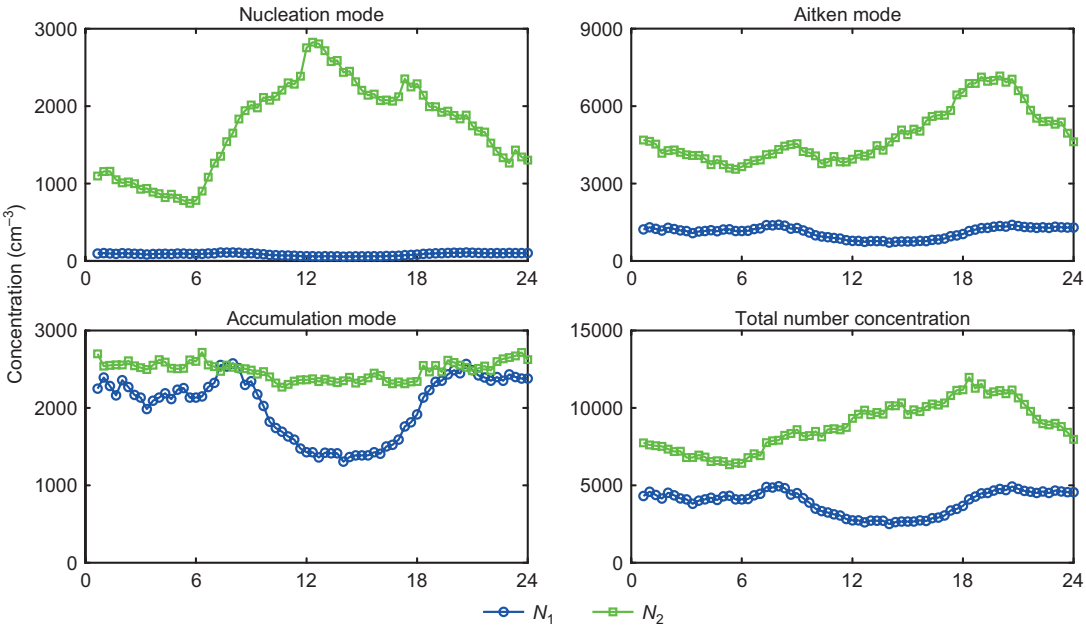

Fig. 5. Same as Fig. 4, except for the SORPES station.

scatter plot (S_1 in Eq. 1 and Figs. 1–3) represents primary particles containing a BC core, a crude estimate of the size of this core can be obtained. Assuming further that the core is spherical, its diameter can be written as:

$$D_p = [6/(\pi S_1 \rho)]^{1/3} \quad (3)$$

where ρ is the core density. Park *et al*. (2004) showed that the density of non-volatile components of diesel soot is 1.7–1.8 g cm^{-3} and that the bulk density of a BC-sulfuric acid mixture has been estimated to be ≈ 1.7 g cm^{-3} (Zhang *et al*. 2008). By assuming this density and varying the N_1 *vs*. [BC] slope (i.e. S_1) using the values given in Table 3 for the total particle number concentrations, the diameter of the BC core can be estimated to be in the range of 82–121 nm for the SMEAR II station, and in the range of 80–95 nm for the SORPES station. This size estimate is consistent with general knowledge of BC particle size obtained with more sophisticated methods. For example, Schwarz *et al*. (2008) measured BC size distributions with a single-particle soot photometer (SP2) and found that the mass median diameter (MMD) and geometric standard deviation (σ_g) of these distributions were 170 nm and 1.71, respectively, in an urban air, and 210 nm and 1.55, respectively, in a continental background air. These values yield the number mean BC diameters of 72 nm and 118 nm for urban and continental background air, respectively, when using the Hatch-Choate conversion equations (Hinds 1999). Moteki *et al*. (2007) followed a pollution plume downwind of Tokyo and measured BC size distributions with an SP2 in an aircraft. The resulting MMD and σ_g of the measured distributions were 190 nm and 1.55, respectively, at two hours downwind of Tokyo, and 210 nm and 1.45, respectively, at 14 hours downwind of Tokyo. The corresponding number mean BC diameters are 107 nm and 139 nm.

The particles that were detected when the number concentrations were above the lowest edge of the *N vs*. [BC] scatter plot, i.e. above the line S_1, could also contain a BC core, provided that this core is small. Earlier, we assumed that all the particles that were observed when the number concentrations were above the line S_1 were secondary. However, the color-coding in Fig. 1 shows that there are also particles with a low single-scattering albedo ($\omega_0 < 0.8$) indicative of primary particles above this line. It is possible that these particles represent fresh BC-containing particles that are much smaller than the

above estimated 99 nm. There are, for example, cases of dark particles with $N \approx 10\,000$ cm^{-3} and [BC] ≈ 1 μg m^{-3}. This would yield a count mean diameter of 47 nm for the BC core, which is in reasonable agreement with freshly-emitted BC particle agglomerates (e.g. Zhang *et al*. 2008). Therefore, we repeated the calculation of N_1 and N_2 by subtracting the number concentrations of particles having $\omega_0 < 0.8$ from N_2 and added them to N_1:

$$N_2 = N - S_1 \times [\mathrm{BC}] - N(\omega_0 < 0.8) \quad (3)$$

and

$$N_1 = S_1 \times [\mathrm{BC}] + N(\omega_0 < 0.8) \quad (4)$$

The comparison of the relative contributions of primary and secondary particles calculated this way (Eqs. 3 and 4, Table 5) with our original method (Eqs. 1 and 2, Table 4) shows that the overall conclusion made in the previous section will not change: the majority of particles are still of secondary origin.

We finally investigated how sensitive our results are to the method used to determine the BC concentration (Tables 6 and 7). The values of the slopes S_1 varyied by tens of per cents: at SORPES, for example, the values of S_1 were 1.11×10^6 particles ng(BC)$^{-1}$ and 1.67×10^6 particles ng(BC)$^{-1}$ when using the Weingartner *et al*. (2003) and Arnott *et al*. (2005) corrections, respectively (Table 6). However, while the latter value of S_1 was about 50% greater than the former one, the final result was affected only little. The reason is that when N_1 is calculated with Eq. 1, not only S_1 but also the BC concentration is affected by the same algorithm. As a result, the primary fractions are relatively insensitive to the algorithm used for processing the aethalometer data, the differences being on the order of a few percentage points in our case (Table 7). With the same reasoning, the method is also insensitive to the use of different MAC values.

Conclusions

We investigated the contributions of primary and secondary aerosol production to the size-segregated particle number load by using the black

Table 5. Estimated fraction of primary particles at SMEAR II and SORPES when including the single scattering albedo correction (Eqs. 3 and 4). Only the cases with 1% of the data points locating below the line $S_1 \times$ [BC] are shown. The values obtained for the nucleation mode are very rough estimates (see the main text), so these values are given in parenthesis.

	Nucleation mode	Aitken mode	Accumulation mode	Total number concentration
SMEAR II	(0.11)	0.18	0.25	0.21
SORPES	(0.04)	0.20	0.50	0.33

Table 6. The values of S_1 (10^6 particles ng(BC)$^{-1}$) obtained when using different ways to determine the BC concentration. Only the cases with 1% of the data points locating below the line $S_1 \times$ [BC] are shown.

	Arnott *et al.* (2005)	Collaud Coen *et al.* (2010)	Weingartner *et al.* (2003)	MAAP
SMEAR II				
Nucleation mode	0.021	0.029	0.019	0.015
Aitken mode	0.401	0.469	0.363	0.367
Accumulation mode	0.457	0.506	0.460	0.512
Total number concentration	1.279	1.512	1.201	1.130
SORPES				
Nucleation mode	0.037	0.026	0.022	
Aitken mode	0.473	0.330	0.284	
Accumulation mode	0.890	0.739	0.664	
Total number concentration	1.670	1.260	1.110	

Table 7. Estimated fraction of primary particles based on the values of S_1 in Table 6.

	Arnott *et al.* (2005)	Collaud Coen *et al.* (2010)	Weingartner *et al.* (2003)	MAAP
SMEAR II				
Nucleation mode	0.01	0.01	0.01	0.01
Aitken mode	0.08	0.08	0.08	0.08
Accumulation mode	0.20	0.20	0.22	0.23
Total number concentration	0.13	0.12	0.13	0.12
SORPES				
Nucleation mode	0.04	0.03	0.03	
Aitken mode	0.20	0.16	0.16	
Accumulation mode	0.50	0.49	0.50	
Total number concentration	0.33	0.29	0.30	

carbon concentration as a tracer for primary particles. Our analysis was based on the long-term observations performed at a boreal forest site (SMEAR II in Hyytiälä, Finland) and highly-polluted urban background site (SORPES in Nanjing, China). We found that at the boreal forest site, primary particles contributed only 10%–20% to the total aerosol number load and about 20%–30% to the accumulation mode particle number concentration. The contribution of primary particles to the nucleation and Aitken modes was estimated to be smaller, likely below 10%. In the polluted site affected heavily by anthropogenic sources, the relative fraction of primary particles was greater, yet most of the particles appeared to be of secondary origin even in the accumulation mode.

Our results indicate that the particle number concentrations, and therefore the aerosol number budget, is dominated by the secondary pathways. Even in a highly-polluted environment like Nanjing, secondary aerosol formation is very pronounced during the daytime, and particularly in summer months when the typical BC concentration is of the order of 1 μg m^{-3} (*see* Fig. 3). This result is in line with other studies in China, determined from aerosol chemical composition measurements (e.g. Guo *et al*. 2014, Huang *et al*. 2014). Furthermore, signatures of frequent NPF have been observed in Chinese megacities (e.g. Wu *et al*. 2007, Xiao *et al*. 2015) under conditions where this phenomenon would not be observed in moderately polluted environments (e.g. Nie *et al*. 2014, Kulmala *et al*. 2014, Kulmala 2015). Our analysis demonstrates the importance and effectiveness of making continuous and comprehensive observations, allowing one to explore the validity hypotheses like the one investigated here.

Acknowledgements: The work was partly supported by the European Commission via projects ACTRIS, ACTRIS2 and BACCHUS, Academy of Finland Centre of Excellence (project number 272041) and Nordforsk via Cryosphere-Atmosphere Interactions in a Changing Arctic Climate, CRAICC. This work was partly supported by the National Natural Science Foundation of China (D0512/41422504 and D0512/41305123) and by the Jiangsu Provincial Science Fund (no. BK20140021). The SORPES was supported by the 985 program of the Ministry of Education and by the Collaborative Innovation Center of Climate Change in Jiangsu Provence, China. The authors gratefully acknowledge the technical support of the SMEAR II and SORPES staff.

References

Aalto P., Hämeri K., Becker E., Weber R., Salm J., Mäkelä J.M., Hoell C., O'Dowd C.D., Karlsson H., Hansson H.-C., Väkevä M., Koponen I.K., Buzorius G. & Kulmala M. 2001. Physical characterization of aerosol particles during nucleation events. *Tellus* 53B: 344–358.

Anderson T.L. & Ogren J.A. 1998. Determining aerosol radiative properties using the TSI 3563 integrating nephelometer. *Aerosol Sci. Technol*. 29: 57–69.

Arnott W.P., Hamasha K., Moosmuller H., Sheridan P.J. & Ogren J.A. 2005. Towards aerosol light-absorption measurements with a 7-wavelength aethalometer: evaluation with a photoacoustic instrument and 3-wavelength nephelometer. *Aerosol Sci. Tech*. 39: 17–29.

Bond T.C., Doherty S.J., Fahey D.W., Forster P.M., Berntsen T., DeAngelo B.J., Flanner M.G., Ghan S., Kärcher B., Koch D., Kinne S., Kondo Y., Quinn P.K., Sarofim M.C., Schultz M.G., Schulz M., Venkataraman C., Zhang H., Zhang S., Bellouin N., Guttikunda S.K., Hopke P.K.,

Jacobson M.Z., Kaiser J.W., Klimont Z., Lohmann U., Schwarz J.P., Shindell D., Storelvmo T., Warren S.G. & Zender C.S. 2013. Bounding the role of black carbon in the climate system: a scientific assessment. *J. Geophys. Res.* 118: 5380–5552.

Brines M., Dall'Osto M., Beddows D.C.S., Harrison R.M., Gomez-Moreno F., Nunez L., Artinano B., Costabile F., Gobbi G.P., Salimi F., Morawska L., Sioutas C. & Querol X. 2015. Traffic and nucleation events as main sources of ultrafine particles in high-insolation developed world cities. *Atmos. Chem. Phys.* 15: 5929–5945.

Collaud Coen M., Weingartner E., Apituley A., Ceburnis D., Fierz-Schmidhauser R., Flentje H., Henzing J.S., Jennings S.G., Moerman M., Petzold A., Schmid O. & Baltensperger U. 2010. Minimizing light absorption measurement artifacts of the aethalometer: evaluation of five correction algorithms. *Atmos. Meas. Tech.* 3: 457–474.

Ding A.J., Fu C.B., Yang X.Q., Sun J.N., Zheng L.F., Xie Y.N., Herrmann E., Nie W., Petäjä T., Kerminen V.-M. & Kulmala M. 2013a. Ozone and fine particle in the western Yangtze River Delta: an overview of 1 yr data at the SORPES station. *Atmos. Chem. Phys.* 13: 5813–5830.

Ding A.J., Fu C.B., Yang X.Q., Sun J.N., Petäjä T., Kerminen V.-M., Wang T., Xie Y., Herrmann E., Zheng L.F., Nie W., Liu Q., Wei X.L. & Kulmala M. 2013b. Intense atmospheric pollution modifies weather: a case of mixed biomass burning with fossil fuel combustion pollution in eastern China. *Atmos. Chem. Phys.* 13: 10545–10554.

Docherty K.S., Stone E.A., Ulbrich I.M., DeCarlo P.F., Snyder D.C., Schauer J.J., Peltier R.E., Weber R.J., Murphy S.M., Seinfeld J.H., Grover B.D., Eatough D.J. & Jimenez J.L. 2008. Apportionment of primary and secondary organic aerosols in southern California during the 2005 Study of Organic Aerosols in Riverside (SOAR-1). *Environ. Sci. Technol.* 42: 7655–7662.

Farmer Q., Chen, Kimmel J.R., Docherty K.S., Nemitz E., Artaxo P.A., Cappa C.D., Martin S.T. & Jimenez J.L. 2013. Chemically-resolved particle fluxes over tropical and temperate forests. *Aerosol Sci. Technol.* 47: 818–830.

Fernández-Camacho R., Rodríguez S., de la Rosa J., Sánchez de la Campa A.M., Viana M., Alastuey A. & Querol X. 2010. Ultrafine particle formation in the inland sea breeze airflow in southwest Europe. *Atmos. Chem. Phys.* 10: 9615–9630.

Fountoukis C., Riipinen I., Denier van der Gon H.A.C., Charalampidis P.E., Pilinis C., Wiedensohler A., O'Dowd C., Putaud J.-P., Moerman M. & Pandis S.N. 2012. Simulating ultrafine particle formation in Europe using a regional CTM: contribution of primary emissions versus secondary formation to aerosol number concentrations. *Atmos. Chem. Phys.* 12: 8663–8677.

Gonzáles Y. & Rodríguez S. 2013. A comparative study on the ultrafine particle episodes induced by vehicle exhaust: A crude oil refinery and ship emissions. *Atmos. Res.* 120–121: 43–54.

Gonzáles Y., Rodríguez, S., García J.C.G., Trujillo J.L. & García R. 2011. Ultrafine particles pollution in urban coastal air due to ship emissions. *Atmos. Environ.* 45: 4907–4914.

Guo S., Hu M., Zamora M.L., Peng J., Shang D., Zheng J., Du Z., Wu Z., Shao M., Zeng L., Molina M.J. & Zhang R. 2014. Elucidating severe urban haze formation in China. *Proc. Natl. Acad. Sci. USA* 111: 17373–17378.

Hari P. and Kulmala M. 2005. Station for Measuring Ecosystem-Atmosphere Relations (SMEAR II). *Boreal Env. Res.* 10: 315–322.

Herrmann E., Ding A.J., Kerminen V.-M., Petäjä T., Yang X.Q., Sun J.N., Qi X.M., Manninen H., Hakala J., Nieminen T., Aalto P.P., Kulmala M. & Fu C.B. 2014. Aerosols and nucleation in eastern China: first insights from the new SORPES-NJU station. *Atmos. Chem. Phys.* 14: 2169–2183.

Hinds W.C. 1999. *Aerosol technology — properties, behavior, and measurement of airborne particles*, 2nd ed. Wiley, New York.

Huang R.-J., Zhang Y., Bozzetti C., Ho K.-F., Cao J.-J., Han Y., Daellenback K.R., Slowik J.G., Platt S.M., Canonaco F., Zotter P., Wolf R., Pieber S.M., Burns E.A., Crippa M., Ciarelli G., Piazzalunga A., Schwikowski M., Abbaszade G., Schnelle-Kreis J., Zimmermann R., An Z., Szidat S., Baltensperger U., El Haddad I. & Prevot A.S.H. 2014. High secondary aerosol contribution to particulate pollution during haze events in China. *Nature* 514: 218–222.

Jimenez J.L., Canagaratna M.R., Donahue N.M., Prevot A.S.H., Zhang Q., Kroll J.H., DeCarlo P.F., Allan J.D., Coe H., Ng N.L., Aiken A.C., Docherty K.S., Ulbrich I.M., Grieshop A.P., Robinson A.L., Duplissy J., Smith J.D., Wilson K.R., Lanz V.A., Hueglin C., Sun Y.L., Tian J., Laaksonen A., Raatikainen T., Rautiainen J., Vaattovaara P., Ehn M., Kulmala M., Tomlinson J.M., Collins D.R., Cubison M.J., Dunlea E.J., Huffman J.A., Onasch T.B., Alfarra M.R., Williams P.I., Bower K., Kondo Y., Schneider J., Drewnick F., Borrmann S., Weimer S., Demerijan K., Salcedo D., Cottrell L., Griffin R., Takami A., Miyoshi T., Hatekeyama S., Shimono A., Sun J.Y., Zhang Y.M., Dzepina K., Kimmel J.R., Sueper D., Jayne J.T., Herndon S.C., Trimborn A.M., Williams L.R., Wood E.C., Middlebrook A.M., Kolb C.E., Baltensperger U. & Worsnop D.R. 2009. Evolution of organic aerosols in the atmosphere. *Science* 326: 1525–1529.

Kerminen V.-M., Paramonov M., Anttila T., Riipinen I., Fountoukis C., Korhonen H., Asmi, E., Laakso L., Lihavainen H., Swietlicki E., Svenningsson B., Asmi A., Pandis S. N., Kulmala M. & Petäjä T. 2012. Cloud condensation nuclei production associated with atmospheric nucleation: a synthesis based on existing literature and new results. *Atmos. Chem. Phys.* 12: 12037–12059.

Kleeman M.J., Schauer J.J. & Cass G.R. Size and composition distribution of fine particulate matter emitted from wood burning, meat charbroiling, and cigarettes. *Environ. Sci. Technol.* 33: 3516–3523.

Kulmala M. 2015. Atmospheric chemistry: China's choking cocktail. *Nature* 526: 497–479.

Kulmala M. & Kerminen V.-M. 2008. On the growth of atmospheric nanoparticles. *Atmos. Res.* 90: 132–150.

Kulmala M., Petäjä T., Ehn M., Thornton J., Sipilä M.,

Worsnop D.R. & Kerminen V.-M. 2014. Chemistry of atmospheric nucleation: On the recent advances on precursor characterization and atmospheric cluster composition in connection with atmospheric new particle formation. *Annu. Rev. Phys. Chem.* 65: 21–37.

Kulmala M., Vehkamäki H., Petäjä T., Dal Maso M., Lauri A., Kerminen V.-M., Birmili W. & McMurry P.H. 2004. Formation and growth rates of ultrafine atmospheric particles: A review of observations. *J. Aerosol Sci.* 35: 143–176.

Kulmala M., Riipinen I., Sipilä M., Manninen H.E., Petäjä T., Junninen H., Dal Maso M., Mordas G., Mirme A., Vana M., Hirsikko A., Laakso L., Harrison R.M., Hanson I., Leung C., Lehtinen K.E.J. & Kerminen V.-M. 2007. Towards direct measurement of atmospheric nucleation. *Science* 318: 89–92.

Kulmala M., Kontkanen J., Junninen H., Lehtipalo K., Manninen H.E., Nieminen T., Petäjä T., Sipilä M., Schobesberger S., Rantala P., Franchin A., Jokinen T., Järvinen E., Äijälä M., Kangasluoma J., Hakala J., Aalto P.P., Paasonen P., Mikkilä J., Vanhanen J., Aalto J., Hakola H., Makkonen U., Ruuskanen T., Mauldin R.L.III, Duplissy J., Vehkamäki H., Bäck J., Kortelainen A., Riipinen I., Kurten T., Johnston M.V., Smith J.N., Ehn M., Mentel T.F., Lehtinen K.E.J., Laaksonen A., Kerminen V.-M. & Worsnop D.R. 2013. Direct observations of atmospheric aerosol nucleation. *Science* 339: 943–946.

Makkonen R., Asmi A., Kerminen V.-M., Boy M., Arneth A., Hari P. & Kulmala M. 2012. Air pollution control and decreasing new particle formation lead to strong climate warming. *Atmos. Chem. Phys.* 12: 1515–1524.

Merikanto J., Spracklen D.V., Mann G.W., Pickering S.J. & Carslaw K.S. 2009. Impact of nucleation on global CCN. *Atmos. Chem. Phys.* 9: 8601–8616.

Moteki N., Kondo Y., Miyazaki Y., Takegawa N., Komazaki Y., Kurata G., Shirai T., Blake D.R., Miyakawa T. & Koike M. 2007. Evolution of mixing state of black carbon particles: aircraft measurements over the western Pacific in March 2004. *Geophys. Res. Lett.* 34, L11803, doi:10.1029/2006GL028943.

Müller T., Laborde M., Kassell G. & Wiedensohler A. 2011a. Design and performance of a three-wavelength LED-based total scatter and backscatter integrating nephelometer. *Atmos. Meas. Tech.* 4: 1291–1303.

Müller T., Henzing J.S., De Leeuw G., Wiedensohler A., Alastuey A., Angelov H., Bizjak M., Collaud Coen M., Engström J.E., Gruening C., Hillamo R., Hoffer A., Imre K., Ivanow P., Jennings G., Sun J.Y., Kalivitis N., Karlsson H., Komppula M., Laj P., Li S.-M., Lunder C., Marinoni A., Martins dos Santos S., Moerman M., Nowak A., Ogren J.A., Petzold A., Pichon J.M., Rodríguez S., Sharma S., Sheridan P.J., Teinilä K., Tuch T., Viana M., Virkkula A., Weingartner E., Wilhelm R. & Wang Y.Q. 2011b. Characterization and intercomparison of aerosol absorption photometers: results of two intercomparison workshops. *Atmos. Meas. Tech.* 4: 245–268.

Nie W., Ding A., Wang T., Kerminen V.-M., George C., Xue L., Wang W., Zhang Q., Petäjä T., Qi X., Wang X., Yang X., Fu C. & Kulmala M. 2014. Polluted dust promotes new particle formation and growth. *Sci. Rep.* 4, 6634, doi:10.1038/srep06634.

Paasonen P., Kupiainen K., Klimont Z., Denier van der Gon H., Visshedjik A. & Amann M. 2016. Continental anthropogenic primary particle number emissions, *Atmos. Chem. Phys. Discuss.* 16, doi:10.5194/acp-2015-1023, in review.

Park K., Kittelson D.B., Zachariah M.R. & McMurry P.H. 2004. Measurement of inherent material density of nanoparticle agglomerates. *J. Nanoparticle Res.* 6: 267–272.

Posner L.N. & Pandis S.N. 2015. Sources of ultrafine particles in the Eastern United States. *Atmos. Environ.* 111: 103–112.

Qi X.M., Ding A.J., Nie W., Petäjä T., Kerminen V.-M., Herrmann E., Xie Y.N., Zheng L.F., Manninen H., Aalto P., Sun J.N., Xu Z.N., Chi X.G., Huang X., Boy M., Virkkula A., Yang X.-Q., Fu C.B. & Kulmala M. 2015. Aerosol size distribution and new particle formation in the western Yangtze River Delta of China: 2 years of measurements at the SORPES station. *Atmos. Chem. Phys.* 15: 12445–12464.

Reche C., Querol X., Alastuey A., Viana M., Pey J., Moreno T., Rodríguez S., Gonzalez S., Fernández-Camacho R., Sánchez de la Campa A.M., de la Rosa J., Dall'Osto M., Prévot A.S.H., Hueglin C., Harrison R.M. & Quincey P. 2011. New considerations for PM, Black Carbon and particle number concentration for air quality monitoring across different European cities. *Atmos. Chem. Phys.* 11: 6207–6227.

Reddington C.L., Carslaw K.S., Spracklen D.V., Frontoso M.G., Collins L., Merikanto J., Minikin A., Hamburger T., Coe H., Kulmala M., Aalto P., Flentje H., Plass-Dülmer C., Birmili W., Wiedensohler A., Wehner B., Tuch T., Sonntag A., O'Dowd C.D., Jennings S.G., Dupuy R., Baltensperger U., Weingartner E., Hansson H.-C., Tunved P., Laj P., Sellegri K., Boulon J., Putaud J.-P., Gruening C., Swietlicki E., Roldin P., Henzing J.S., Moerman M., Mihalopoulos N., Kouvarakis G., Ždímal V., Zíková N., Marinoni A., Bonasoni P. & Duchi, R. 2011. Primary versus secondary contributions to particle number concentrations in the European boundary layer. *Atmos. Chem. Phys.* 11: 12007–12036.

Rodríguez S. & Cuevas E. 2007. The contributions of "minimum primary emissions" and "new particle formation enhancements" to the particle number concentration in urban air. *J. Aerosol Sci.* 38: 1207–1219.

Schutgens N.A.J. & Stier P. 2014. A pathway analysis of global aerosol processes. *Atmos. Chem. Phys.* 14: 11657–11686.

Schwarz J.P., Gao R.S., Spackman J.R., Watts L.A., Thomson D.S., Fahey D.W., Ryerson T.B., Peischl J., Holloway J.S., Trainer M., Frost G.J., Baynard T., Lack D.A., de Gouw J.A., Warneke C. & Del Negro L.A. 2008. Measurement of the mixing state, mass, and optical size of individual black carbon particles in urban and biomass burning emissions. *Geophys. Res. Lett.* 35, L13810, doi:10.1029/2008GL033968.

Spracklen D.V., Carslaw K.S., Merikanto J., Mann G.W., Reddington C.L., Pickering S., Ogren J.A., Andrews E., Baltensperger U., Weingartner E., Boy M., Kulmala

M., Laakso L., Lihavainen H., Kivekäs N., Komppula M., Mihalopoulos N., Kouvarakis G., Jennings S.G., O'Dowd C., Birmili W., Wiedensohler A., Weller R., Gras J., Laj P., Sellegri K., Bonn B., Krejci R., Laaksonen A., Hamed A., Minikin A., Harrison R.M., Talbot R. & Sun J. 2010. Explaining global surface aerosol number concentrations in terms of primary emissions and particle formation. *Atmos. Chem. Phys.* 10: 4775–4793.

Tsigaridis K., Daskalakis N., Kanakidou M., Adams P.J., Artaxo P., Bahadur R., Balkanski Y., Bauer S.E., Bellouin N., Benedetti A., Bergman T., Berntsen T.K., Beukes J.P., Bian H., Carslaw K.S., Chin M., Curci G., Diehl T., Easter R.C., Ghan S.J., Gong S.L., Hodzic A., Hoyle C.R., Iversen T., Jathar S., Jimenez J.L., Kaiser J.W., Kirkevåg A., Koch D., Kokkola H., Lee Y.H, Lin G., Liu X., Luo G., Ma X., Mann G.W., Mihalopoulos N., Morcrette J.-J., Müller J.-F., Myhre G., Myriokefalitakis S., Ng N.L., O'Donnell D., Penner J.E., Pozzoli L., Pringle K.J., Russell L.M., Schulz M., Sciare J., Seland Ø., Shindell D.T., Sillman S., Skeie R.B., Spracklen D., Stavrakou T., Steenrod, S.D., Takemura T., Tiitta P., Tilmes S., Tost H., van Noije T., van Zyl P.G., von Salzen K., Yu F., Wang Z., Zaveri R.A., Zhang H., Zhang K., Zhang Q. & Zhang X. 2014. The AeroCom evaluation and intercomparison of organic aerosol in global models. *Atmos. Chem. Phys.* 14: 10845–10895.

Virkkula A., Mäkelä T., Yli-Tuomi T., Hirsikko A., Koponen I.K., Hämeri K. & Hillamo R. 2007. A simple procedure for correcting loading effects of aethalometer data. *J. Air Waste Manag. Assoc.* 57: 1214–1222.

Virkkula A., Backman J., Aalto P.P., Hulkkonen M., Riuttanen L., Nieminen T., Dal Maso M., Sogacheva L., De Leeuw G. & Kulmala M. 2011. Seasonal cycle, size dependencies, and source analyses of aerosol optical properties at the SMEAR II measurement station in Hyytiälä, Finland. *Atmos. Chem. Phys.* 11: 4445–4468.

Virkkula A., Chi X., Ding A., Shen Y., Nie W., Qi X., Zheng L., Huang X., Xie Y., Wang J., Petäjä T. & Kulmala M. 2015. On the interpretation of the loading correction of the aethalometer. *Atmos. Meas. Tech.* 8: 4415–4427.

Weingartner E., Saathoff H., Schnaiter M., Streit N., Bitnar B. & Baltensperger U. 2003. Absorption of light by soot particles: determination of the absorption coefficient by means of aethalometers. *J. Aerosol Sci.* 34: 1445–1463.

WMO. 2013. *WMO/GAW Aerosol Measurement Procedures Guidelines and Recommendations*, WMO TD No. 1178 – GAW Report No. 153, World Meteorological Organization, Geneva, Switzerland.

Wu Z., Hu M., Liu S., Wehner B., Bauer S., Massling A., Wiedensohler A., Petäjä T., Dal Maso M. & Kulmala M. 2007. New particle formation in Beijing, China: Statistical analysis of a 1-year data set. *J. Geophys. Res.* 112, D09209, doi:10.1029/2006JD007406.

Xiao S., Wang M.Y., Yao L., Kulmala M., Zhou B., Yang X., Chen J.M., Wang D.F., Fu Q.Y., Worsnop D.R. & Wang L. 2015. Strong atmospheric new particle formation in winter in urban Shanghai. China. *Atmos. Chem. Phys.* 15: 1769–1781.

Xie Y., Ding A.J., Nie W., Mao H., Qi X., Huang X., Xu Z., Kerminen V.-M. Petaja T., Chi X., Virkkula A., Boy M., Xue L., Guo J., Sun J., Yang X., Kulmala M. & Fu C. 2015. Enhanced sulfate formation by nitrogen dioxide: Implications from *in situ* observations at the SORPES station. *J. Geophys. Res.* 120: 12679–12694.

Yatavelli R.L.N, Mohr C., Stark C., Day D.A., Thompson S.L., Lopez-Hilfiker F.D., Campuzano-Jost P., Palm B.B., Vogel A.L., Hoffmann T., Heikkinen L., Äijälä M., Ng N.L., Kimmel J.R., Canagaratna M.R., Ehn M., Junninen H., Cubison M.J., Petäjä T., Kulmala M., Jayne J.T., Worsnop D.R. & Jimenez J.L. 2015. Estimating the contribution of organic acids to northern hemispheric continental organic aerosol. *Geophys. Res. Lett.* 42: 6084–6090.

Yu F., Luo G., Bates T.S., Anderson B., Clarke A., Kapustin V., Yantosca R.M., Wnag Y. & Wu S. 2010. Spatial distributions of particle number concentrations in the global troposphere: simulations, observations, and implications for nucleation mechanisms. *J. Geophys. Res.* 115, D17205, doi:10.1029/2009JD013473.

Zhang R., Khalizov A.F., Pagels J., Zhang D., Xue H. & McMurry P.H. 2008. Variability in morphology, hygroscopicity, and optical properties of soot aerosols during atmospheric processing. *Proc. Natl. Acad. Sci. USA* 105: 10291–10296.